PROCEEDINGS OF SPIE

SPIEDigitalLibrary.org/conference-proceedings-of-spie

Microcapillary imaging of lamina cribrosa in porcine eyes using photoacoustic microscopy

Mohesh Moothanchery, Thanadet Chuangsuwanich, Alvan Tsz Chung Yan, Leopold Schmetterer, Michael J. A. Girard, et al.

Mohesh Moothanchery, Thanadet Chuangsuwanich, Alvan Tsz Chung Yan, Leopold Schmetterer, Michael J. A. Girard, Manojit Pramanik, "Microcapillary imaging of lamina cribrosa in porcine eyes using photoacoustic microscopy," Proc. SPIE 10494, Photons Plus Ultrasound: Imaging and Sensing 2018, 104945Q (19 February 2018); doi: 10.1117/12.2287825

SPIE.

Event: SPIE BiOS, 2018, San Francisco, California, United States

Downloaded From: https://www.spiedigitallibrary.org/conference-proceedings-of-spie on 11/14/2018 Terms of Use: https://www.spiedigitallibrary.org/terms-of-use

Microcapillary imaging of Lamina Cribrosa in Porcine Eyes using Photoacoustic Microscopy

Mohesh Moothanchery[1,2], Thanadet Chuangsuwanich[3], Alvan Tsz Chung Yan[3], Leopold Schmetterer[4,5,6,7,8], Michael J. A. Girard[3,5], and Manojit Pramanik[1*]

[1]School of Chemical and Biomedical Engineering, Nanyang Technological University, 62 Nanyang Drive, Singapore 637459
[2]Currently at Singapore Bioimaging Consortium, Agency for Science Technology and Research, 11 Biopolis Way, Singapore 138667
[3]Opthalmic Engineering & Innovation Laboratory, Department of Biomedical Engineering, National University of Singapore, Singapore
[4]Lee Kong Chian School of Medicine, Nanyang Technological University, 59 Nanyang Drive, Singapore 637459
[5]Singapore Eye Research Institute, Singapore National Eye Centre, Singapore
[6]Visual Science Academic Clinical Programme, Duke-NUS, Singapore
[7]Department of Clinical Pharmacology, Medical University of Vienna, Austria
[8]Center of Medical Physics and Biomedical Engineering, Medical University of Vienna, Austria

ABSTRACT

In order to understand the pathophysiology of glaucoma, Lamina cribrosa (LC) perfusion needs to be the subject of thorough investigation. It is currently difficult to obtain high resolution images of the embedded microcapillary network of the LC using conventional imaging techniques. In this study, an optical resolution photoacoustic microscopy (OR-PAM) system was used for imaging lamina cribrosa of an *ex vivo* porcine eye. Extrinsic contrast agent was used to perfuse the eye via its ciliary arteries. The OR-PAM system have a lateral resolution of 4 μm and an axial resolution of 30 μm. The high resolution system could able resolve a perfused LC microcapillary network to show vascular structure within the LC thickness. OR-PAM could be a promising imaging modality to study the LC perfusion and hence could be used to elucidate the hemodynamic aspect of glaucoma.

Keywords: photoacoustic imaging, optic nerve head, lamina cribrosa, microcapillary, glaucoma

1. Introduction

Open angle glaucoma (OAG) is an optic neuropathy disease which is characterized by a progressive loss of retinal ganglion cell (RGC), particularly at the optic nerve head (ONH). Even though the biomechanical aspects of glaucoma have been investigated comprehensively, there is not much evidences to support the vascular hypothesis. This is mainly due to the limitations of current imaging modalities to capture the complex microcapillary network inside the structure called the lamina cribrosa (LC). LC is located deep in the ONH, the site where RGC death occurs. LC consists of microcapillaries that are embedded inside the collagen rich tissue which provides structural support and perfusion to the RGC [1]. The location of LC and the embedment of the microcapillary severely limits the ability of conventional optical imaging modalities to study the microcapillary both *in vivo* and *ex vivo*.

* E-mail: manojit@ntu.edu.sg

Photons Plus Ultrasound: Imaging and Sensing 2018, edited by Alexander A. Oraevsky, Lihong V. Wang, Proc. of SPIE Vol. 10494, 104945Q · © 2018 SPIE · CCC code: 1605-7422/18/$18 · doi: 10.1117/12.2287825

Downloaded From: https://www.spiedigitallibrary.org/conference-proceedings-of-spie on 11/14/2018
Terms of Use: https://www.spiedigitallibrary.org/terms-of-use

Photoacoustic (PA) imaging has made significant advancements over the last decade [2-5]. PA imaging combines optical absorption with acoustic detection, reaping the benefits of both modalities it can produce high resolution images with relatively deep penetration depth. PA imaging achieves contrast by using short burst of electromagnetic (EM) waves which is absorbed to a varying degree by different components of the tissue. The tissue then acts as an acoustic source as it absorbs the energy and undergoes thermoelastic expansion, producing detectable ultrasound. PA imaging is particularly useful in the study of blood flow in embedded microcapillary since hemoglobin absorbs EM pulse and acts as an intrinsic contrast agent.[6] PA imaging has found a wide range of applications, such as cancer detection [7], perfusion study [8] and structural imaging of the brain.[9, 10]. We used an optical resolution photoacoustic microscopy (OR-PAM) system [11] to study the perfusion of the LC in enucleated porcine eyes. We obtained high resolution images of isolated LC (post-perfusion) using OR-PAM with a lateral resolution of 4.2 μm. This is the first study to image the lamina cribrosa microcapillary in detail and it can be a basis of further studies to elucidate the role of blood flow in glaucoma disease.

2. Experimental set up

2.1 Optical resolution photoacoustic microscopy system

The schematic of the OR-PAM is shown in Fig. 1 and was previously described in detail [11, 12]. This OR-PAM system consist of a nanosecond Nd-YAG pump laser and a tunable dye laser. The laser output was reshaped by an iris and spatially filtered by a condenser lens, CL and pinhole, PH. The attenuated beam through a v neutral density filter, NDF was launched on to a single-mode fiber, SMF using a fiber coupler, FC. The output beam from the SMF was collimated by an Achromatic lens, L1 reflected by a stationary elliptical mirror, M and focused by another identical Achromatic lens, L3. The beam then passed through an optoacoustic beam combiner consisting of a right-angled prism, RA and a rhomboid prism, RP with a layer of silicon oil, SO in between. The silicon oil layer acts as optically transparent and acoustically reflective film. An acoustic lens, AL provided acoustic focusing (focal diameter ~46 μm) was attached at the bottom of the rhomboid prism. The ultrasonic transducer, 50 MHz center frequency was placed on top of the rhomboid. To maximize the detection sensitivity, the optical and acoustic foci were aligned confocally. The laser repetition rate for the OR-PAM was set to 5 kHz and the laser energy at focus can be varied up to 200 nJ per pulse.

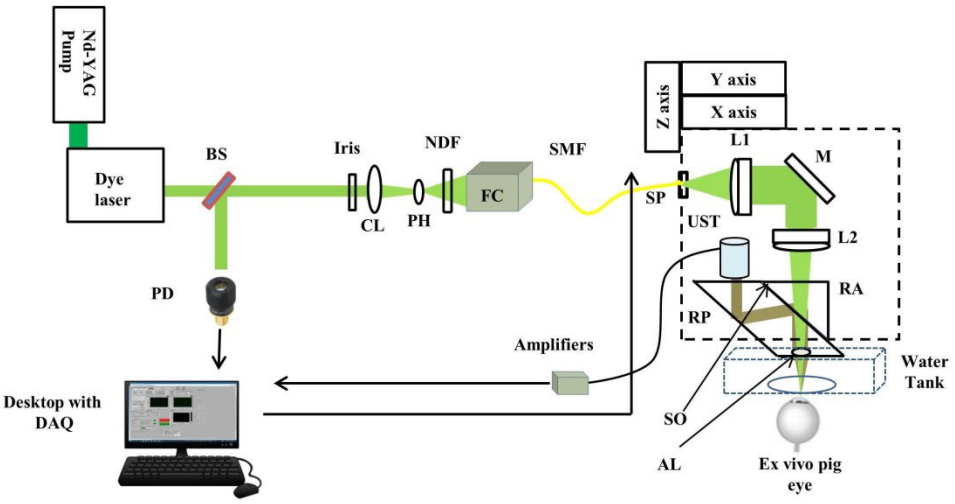

Fig.1. Schematic of the OR-PAM imaging system. BS - Beam Sampler, NDF - Neutral density filter, PD - photodiode, CL - Condenser lens, PH - Pinhole, FC - Fiber coupler, SMF - Single mode fiber, SP - Slip plate, DAQ - Data acquisition card, L1&L2 - Achromatic doublet, , M – Mirror, RA - Right angle prism, RP - Rhomboid prism, UST - Ultrasound transducer, AL - Acoustic lens, SO - Silicon oil.

Downloaded From: https://www.spiedigitallibrary.org/conference-proceedings-of-spie on 11/14/2018
Terms of Use: https://www.spiedigitallibrary.org/terms-of-use

The OR-AR-PAM scanner head was attached to a 3-axis motorized stage. For photoacoustic imaging the bottom of the OR-PAM scanner head was submerged in a water-filled tank. An imaging window of 7 cm x 7 cm was opened in the bottom of the tank and sealed with a polyethylene membrane for optical and acoustic transmission. The PA signal acquired by the UST was amplified by two amplifiers each having 24 dB gain, and was recorded using a data acquisition card, DAQ in a desktop. The scanning and data acquisition was controlled using Labview software. Two-dimensional continuous raster scanning of the imaging head was used during image acquisition. The time-resolved PA signals were multiplied by speed of sound (1540 m/s) to obtain an A-line. Multiple A-lines was captured during the continuous motion of the Y stage will produce the 2-dimensional B-scan. Multiple B-scans of the imaging area were captured and stored in the computer.

The synchronization of the data acquisition and the stage motion was controlled through the signal from a photodiode, PD. A beamsampler, BS was placed in front of the laser beam diverted a small portion of the beam (5%) to the PD. A neutral density filter, NDF 1 was placed in front of the PD to control the energy falling on the PD. The PD signal was also used for compensating pulse to pulse variations during data acquisition. All experiments were done at a laser wavelength of 570 nm in this work. The lateral resolution of the OR-PAM and AR-PAM was 4 µm and 45 µm respectively. The use of photopolymer material [13, 14] for making transparent 3D casing and the use of a MEMS scanner [15, 16] can improve the footprint of the system for clinical applications.

2.2 Ex-vio perfusion of porcine eyes

Fresh porcine eyes (within 24 hours of death) was used for the experiments. A syringe pump with adjustable flow rate to drive the flow was used for the perfusion system. A pressure gauge (15 Psi Crystal XP2i) was used to monitor and record the perfusion pressure. A Y-shaped connector using Tygon Microbore Autoanalysis tube with an inner diameter of 1.27 mm was used to direct the flow and a 27G hypodermic needle to cannulate the arteries. A 50 mL syringe was used as a reservoir. We used artificial blue color dye (E133) with 4 drops of dye used per 50 mL of water as the contrast agents for this experiment.

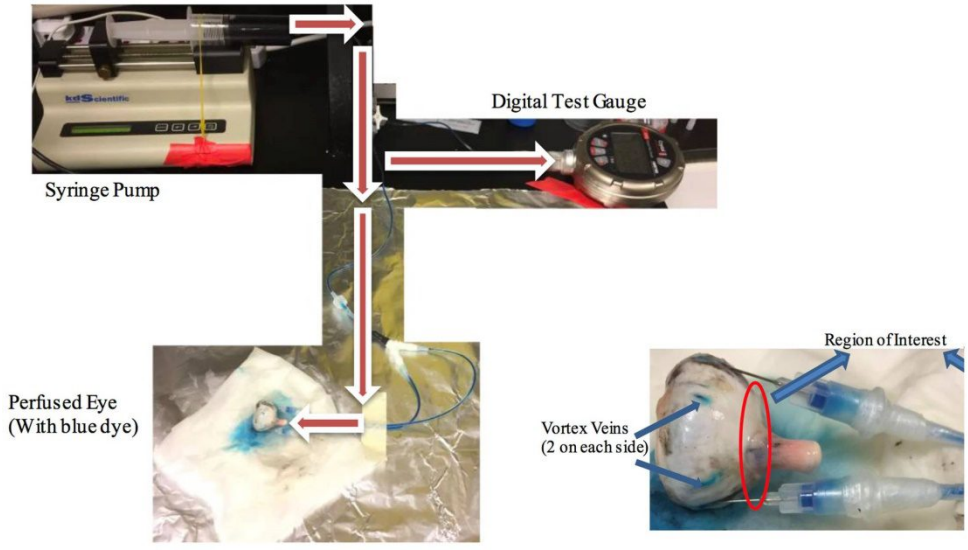

Fig. 2 (a) Schematic of a perfusion system, consisting of a variable syringe pump (with 50 mL Terumo syringe), 1.27 mm Tygon Microbore Autoanalysis tube, a digital test gauge and two 27G needles cannulated to the ciliary arteries. (b) Red dotted-circle is the region of interest (ONH), two blue arrows point to the vortex veins.

Downloaded From: https://www.spiedigitallibrary.org/conference-proceedings-of-spie on 11/14/2018
Terms of Use: https://www.spiedigitallibrary.org/terms-of-use

The two ciliary arteries, one each on opposite side of the globe was cannulated by carefully inserting 27G needles under a microscope. We ensured that the needle did not penetrate the sclera during the process. The perfusion was done with constant flow rate of 4 mL/min; this rate was deduced from numerous trials to obtain the stable perfusion pressure (approximately 40 mmHg) and a constant outflow from the vortex vein (Fig. 2). The perfusion time was at least 30 minutes for each successful perfusion. We used both the contrast agents for high resolution OR-PAM imaging. The perfused eyes were then incised to isolate the area around the ONH for OR-PAM imaging. We made a circular cut of approximately 1 cm in diameter with the LC being roughly in the center. The choroid layer was preserved.

3. Results and discussion

Imaging of perfused LCs using OR-PAM

We obtained high resolution images, with a lateral resolution of 4 µm, in perfused LCs using OR-PAM. Figure 3(a) shows the OR-PAM image of a perfused LC covering the area of 3.5 mm by 3.5 mm with a step size of 4 µm along both axis. Figure 3(b) shows the OR-PAM image of a white dotted area in Fig. 3a (scan area 2 mm by 2 mm) with similar step size as before. It was observed that the eye that was perfused with a blue dye solution, we observed a strong signal from the LC, revealing its collagen beam which contains capillary network. Porcine LCs exhibited an oval shape with an average major axis length of 2.2 mm and an average minor axis length of 1.7 mm and 350 µm depth.

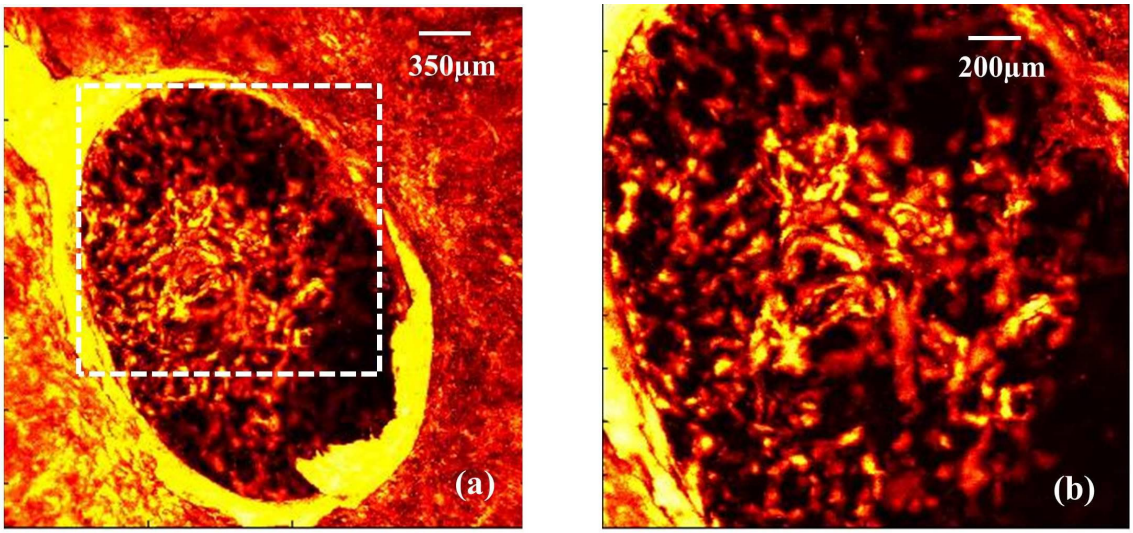

Fig. 3 OR-PAM maximum Amplitude projection images (a) perfused LC with blue dye as a contrast agent (b) White dotted area in (a).

Fig. 4 shows the depth resolved maximum amplitude projection images of the LC microcapillary netwroks. The OR-PAM imaging could clearly resolve microcappliary network at each depth from the surface. In this study we have demonstrated the use of an OR-PAM system to image LC microcapillary. This study attempts to image the LC's structure and microcapillary network which could be the key to elucidating the glaucoma disease. We obtained high resolution images of the perfused LC using OR-PAM and a blue dye as contrast agents. The contrast agents was readily absorbed by the excitation laser (570 nm) and provided strong ultrasound signals. When no contrast agent was used, there was no signal emitted from the LC and this acted as our negative control. Strong signal could still be observed in Figure 3a and 3b from region outside the ONH, since the inner-sclera is covered by a dark melanin from the retinal endothelium.[17]. The OR-PAM provides a uniform image with a clearer defining feature.

Downloaded From: https://www.spiedigitallibrary.org/conference-proceedings-of-spie on 11/14/2018
Terms of Use: https://www.spiedigitallibrary.org/terms-of-use

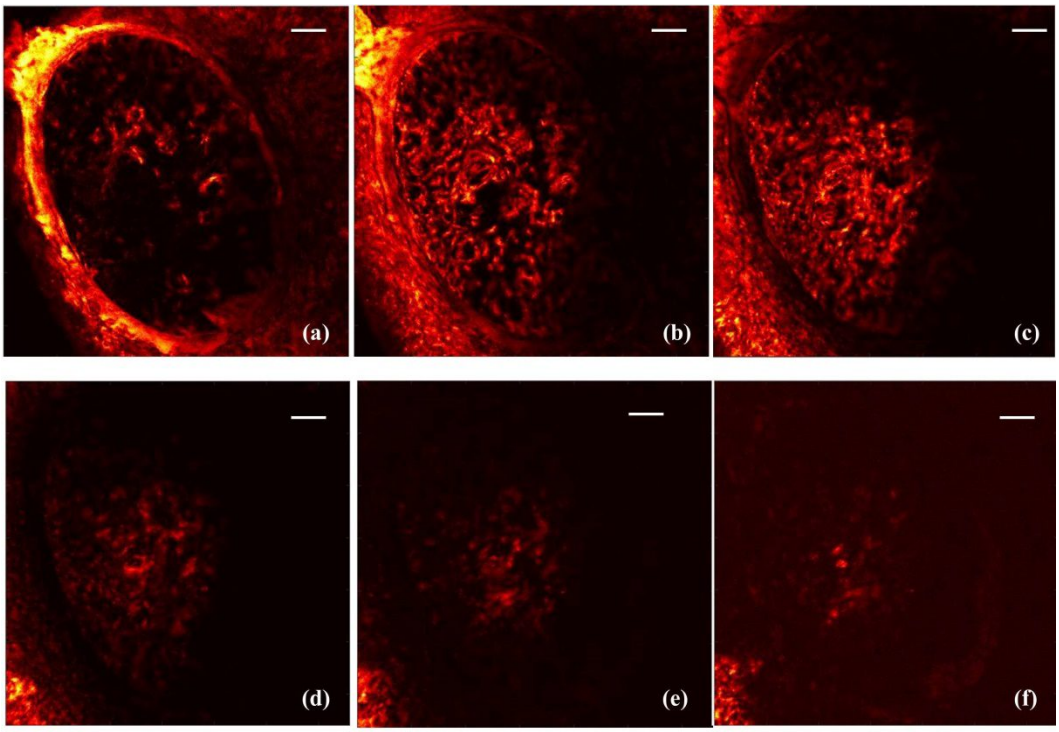

Fig. 4 OR-PAM depth resolved maximum Amplitude projection images (a) 0-60 µm (b) 61-120 µm (c) 121-180 µm (d) 181-240 µm (b) 241-300 µm (c) 301-360 µm from the skin surface after gold coated microneedles insertion. Scale bar corresponds to 350 µm.

4. Conclusion

In conclusion, we presented an ex-*vivo* experimental set-up to study and image LC. We have established that photoacoustic is a powerful imaging modality that can obtain high-resolution perfusion images of the LC, with good depth information and good sensitivity. The current set-up could be used in future studies to investigate the effects of various factors on the LC and ONH blood flow in general. For instance, investigating how an increase in intraocular pressure (IOP) results in a change in LC perfusion would be of great importance to our understanding of glaucoma disease.

Acknowledgements

The authors would also like to acknowledge the financial support from a Tier 2 grant funded by the Ministry of Education in Singapore (ARC2/15: M4020238; MP) and from a National University of Singapore Young Investigator Award (NUSYIA_FY13_P03, R-397-000-174-133; Girard). Authors have no relevant financial interests in the manuscript and no other potential conflicts of interest to disclose.

REFERENCES

[1] C. F. Burgoyne, "A biomechanical paradigm for axonal insult within the optic nerve head in aging and glaucoma," Experimental Eye Research, 93(2), 120-132 (2011).

Downloaded From: https://www.spiedigitallibrary.org/conference-proceedings-of-spie on 11/14/2018
Terms of Use: https://www.spiedigitallibrary.org/terms-of-use

[2] M. Xu, and L. V. Wang, "Photoacoustic imaging in biomedicine," Review of Scientific Instruments, 77(4), 041101 (2006).
[3] M. Moothanchery, A. Sharma, and M. Pramanik, "Switchable Acoustic and Optical Resolution Photoacoustic Microscopy for in vivo small-animal blood vasculature imaging," Journal of Visualized Experiments(124), e55810 (2017).
[4] P. K. Upputuri, and M. Pramanik, "Recent advances toward preclinical and clinical translation of photoacoustic tomography: a review," Journal of Biomedical Optics, 22(4), 041006 (2017).
[5] R. Bi, G. Balasundaram, S. Jeon *et al.*, "Photoacoustic microscopy for evaluating combretastatin A4 phosphate induced vascular disruption in orthotopic glioma," Journal of Biophotonics, (2018)(published).
[6] A. Grinvald, E. Lieke, R. D. Frostig *et al.*, "Functional architecture of cortex revealed by optical imaging of intrinsic signals," Nature, 324(6095), 361-364 (1986).
[7] M. Mehrmohammadi, S. J. Yoon, D. Yeager *et al.*, "Photoacoustic Imaging for Cancer Detection and Staging," Current molecular imaging, 2(1), 89-105 (2013).
[8] H. F. Zhang, K. Maslov, G. Stoica *et al.*, "Functional photoacoustic microscopy for high-resolution and noninvasive in vivo imaging," Nature biotechnology, 24(7), 848-851 (2006).
[9] J. Yao, and L. V. Wang, "Photoacoustic brain imaging: from microscopic to macroscopic scales," Neurophotonics, 1(1), 011003-011003 (2014).
[10] P. K. Upputuri, and M. Pramanik, "Dynamic in vivo imaging of small animal brain using pulsed laser diode-based photoacoustic tomography system," Journal of Biomedical Optics, 22(9), 090501 (2017).
[11] M. Moothanchery, R. Z. Seeni, C. Xu *et al.*, "In vivo studies of transdermal nanoparticle delivery with microneedles using photoacoustic microscopy," Biomedical Optics Express, 8(12), 5483-5492 (2017).
[12] M. Moothanchery, and M. Pramanik, "Performance Characterization of a Switchable Acoustic Resolution and Optical Resolution Photoacoustic Microscopy System," Sensors, 17(2), 357 (2017).
[13] M. Moothanchery, V. Bavigadda, M. Pramanik *et al.*, "Application of Phase Shifting Electronic Speckle Pattern Interferometry in Studies of Photoinduced Shrinkage of Photopolymer layers," Optics Express, 25(9), 9647-9653 (2017).
[14] M. Moothanchery, I. Naydenova, and V. Toal, "Studies of shrinkage as a result of holographic recording in acrylamide-based photopolymer film," Applied Physics A, 104(3), 899-902 (2011).
[15] K. Park, J. Y. Kim, C. Lee *et al.*, "Handheld Photoacoustic Microscopy Probe," Scientific Reports, 7(1), 13359 (2017).
[16] M. Moothanchery, R. Bi, J. Y. Kim *et al.*, "Optical Resolution Photoacoustic Microscopy Based on Multimode Fibers," Biomedical Optics Express, (2018)(accepted).
[17] C. W. Spraul, G. E. Lang, and H. E. Grossniklaus, "Morphometric analysis of the choroid, Bruch's membrane, and retinal pigment epithelium in eyes with age-related macular degeneration," Investigative ophthalmology & visual science, 37(13), 2724-2735 (1996).

Downloaded From: https://www.spiedigitallibrary.org/conference-proceedings-of-spie on 11/14/2018
Terms of Use: https://www.spiedigitallibrary.org/terms-of-use